

Soret separation in a binary liquid mixture near its critical temperature^{*}

J.C. Legros^{1,3,a}, Yu. Gaponenko¹, T. Lyubimova², and V. Shevtsova¹

¹ MRC, EP CP-165/62, Université Libre de Bruxelles (ULB), av. F.D. Roosevelt, 50, Brussels, 1050 Belgium

² Institute of Continuous Media Mechanics UB RAS, 1, Koroleva str., 614013 Perm, Russia

³ Tomsk Polytechnic University, Tomsk, Russia

Received 15 July 2014 and Received in final form 3 September 2014

Published online: 3 October 2014 – © EDP Sciences / Società Italiana di Fisica / Springer-Verlag 2014

Abstract. The values of transport coefficients near a critical point are typically enhanced compared to the values in the classical region far away from a critical point. We report on the impact of the asymptotic behavior of the mass diffusion near the critical region on the Soret separation of the components in a model binary mixture. Concentration patterns are numerically investigated in the case of a spatially varying temperature. The Soret separation in ordinary mixture leads to the establishing of a linear concentration distribution in a steady state. The presence of the critical point redistributes the concentration field, it creates a thin layer with sharp concentration change at the critical region which can be seen as a horizontal plateau on vertical profiles. Large concentration gradients are established across this layer. The analysis showed that the kinetic of the separation significantly depends on whether the critical temperature is inside or outside of the applied temperature region, which is $T_{\text{cold}} \leq T \leq T_{\text{hot}}$. Critical separation road is suggested for the case when T_{cr} is located inside this region, $T_{\text{cold}} \leq T_{\text{cr}} \leq T_{\text{hot}}$.

1 Introduction

Thermodiffusion (also called thermal diffusion or Soret effect) is a molecular transport of substance in response to a thermal gradient. Concentration gradients appear in an originally uniform mixture and produce molecular diffusion, which aims at eliminating concentration variations. A steady state is reached when the separating effect of thermodiffusion is balanced by the remixing effect of mass diffusion. Then, in steady state the mass flux \mathbf{J}_C vanishes

$$\mathbf{J}_C = -\rho_0[D\nabla C + D_T C(1-C)\nabla T] = 0, \quad (1)$$

$$\nabla C = -S_T C(1-C)\nabla T. \quad (2)$$

Here D is the mass diffusion coefficient, D_T is the thermodiffusion coefficient and $S_T = D_T/D$ is the Soret coefficient. In a linear approach performed in the frame of the thermodynamic of irreversible process, the diffusion and thermodiffusion coefficients are supposed to be constant or weakly dependent on temperature and concentration. When approaching the critical region this simplification cannot be valid. The main effect near the critical point is

the critical slowing down, *i.e.*, the increase of the relaxation time in the system to reach equilibrium. The principle of critical-point universality requires that the critical behavior of binary fluid mixtures be in the same universality class as that of one-component fluids [1–3].

When a binary liquid mixture approaches the critical point, the amplitude of the fluctuations grows according to characteristic power laws. Let us denote the distance from critical point as

$$\epsilon = (T - T_{\text{cr}})/T_{\text{cr}}.$$

The mass diffusion D tends to zero when the temperature is approaching the critical region. There are several experimental results confirming this theoretical prediction. For example, measurements of the diffusion coefficients in critical mixture aniline-cyclohexane [4] provided scaling $D = D_0\epsilon^{0.61}$.

The experimental techniques to measure Soret and diffusion coefficients in ordinary mixtures are continuously advancing [5, 6] while much less works have been dedicated to thermodiffusion in a mixture with critical point. The measurements near the *consolute* critical point of the aniline-cyclohexane mixture by Giglio and Vendramini [7] confirmed the earlier obtained trends by Bergé and Dubois [4] for mass diffusion and indicated that the Soret coefficient diverges as a function of ϵ , with a critical exponent close to that of the long-range correlation

^{*} Contribution to the Topical Issue “Thermal non-equilibrium phenomena in multi-component fluids” edited by Fabrizio Crocco and Henri Bataller.

^a e-mail: jclegr@ulb.ac.be

length, while D_T is practically constant. It suggests that the Soret coefficient $S_T = D_T/D$ may even diverge at the critical point. Presently, the active experimental study of the ternary mixture with consolute point are conducted in the frame DCMIX (Diffusion Coefficients in MIXtures) program of European Space Agency [8, 9].

The only known experiments on thermodiffusion near the critical *plait* point by Rutherford and Roof [10] are dated back to the '50s. They performed measurements at two compositions of methane-n-butane mixture at five different temperatures. The authors reported about a strong increase of the Soret coefficient (thermodiffusion factor in their definition) approaching the critical temperature for both compositions.

Using thermogravitational column, Ecenarro *et al.* [11] studied separation of component as a function of composition near the *plait* critical point. In the system, in which the component densities are very different (nitrobenzene + n-hexane), they observed large separations near the critical composition. In the system with similar densities of the pure components (isobutyric acid + water) no separation was observed.

In light of the experimental results available, it is desirable to analyze the evolution of the Soret separation in course of time. It seems that such experiments have so far received limited attention on theoretical and numerical sides. The present work is therefore motivated by the lack of investigations of the dynamics of a binary mixture in the critical region with the presence of a temperature gradient. We have performed a numerical study of the kinetic of the Soret separation in a model binary mixture near its critical *plait* point.

The paper is organized as follows. First, we construct a simple numerical model. The mathematical formulation and the numerical scheme are discussed in sect. 2. Using this model, we examine the concentration field and dynamics of Soret separation as a function of the location of critical temperature with respect to the temperature of bounding walls.

2 Problem description and formulation

We examine mass transport in a cubic Soret cell filled with a binary mixture. A sketch of the cell and coordinate system are shown in fig. 1 which corresponds to the typical experimental configuration [12]. The horizontal walls of the cell, let us call them as bottom and top walls, are kept at constant temperatures T_{cold} and T_{hot} , respectively. The mean temperature is defined as $T_{\text{mean}} = (T_{\text{hot}} - T_{\text{cold}})/2$. An imposed temperature difference $\Delta T = T_{\text{hot}} - T_{\text{cold}}$ is kept constant, $\Delta T = 3$ K. The temperature $T_0 = 298$ K, is chosen to be the reference temperature at which all the physical properties of the liquid mixture are fixed. The physical properties of the model liquid are listed in table 1 which correspond, for definiteness, to ordinary water-isopropanol mixture. The critical temperature is prescribed to be $T_{\text{cr}} = 301$ K.

The working liquid is placed in a cubic cell of internal size $L = 10$ mm. Let us chose C as the mass fraction

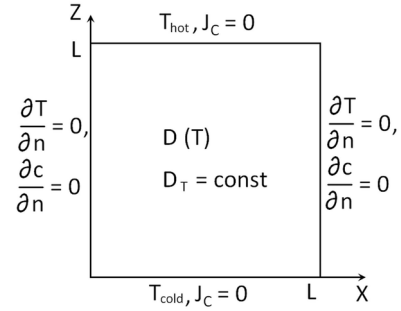


Fig. 1. Schematic of a cubic cell of height L and coordinate system.

Table 1. Physical properties of the model mixture at 298 K (similar to 50%water-50%IPA): density ρ , thermal diffusivity χ and diffusion D and Soret S_T coefficients.

ρ (kg/m ³)	χ (10 ⁻⁷ m ² /s)	D_0 (10 ⁻¹⁰ m ² /s)	S_T (10 ⁻³ K ⁻¹)	T_{cr} (K)	ΔT (K)
902.4	0.85	1.6	5.87	301	3

of one component in binary mixture then the mass fraction of the other component will be $(1 - C)$. Hereafter in a model binary mixture we choose C as mass fraction of the denser component, and C_0 is its initial concentration in the mixture. When pressure diffusion is negligible, the diffusion flux \mathbf{J}_C is driven by concentration and temperature gradients. Then the equations of heat and mass transport can be written as

$$\partial_t T = \chi \nabla^2 T, \quad (3)$$

$$\partial_t C = \nabla(D(T)\nabla C) + C_0(1 - C_0) D_T \nabla^2 T, \quad (4)$$

The typical approximation for such a class of problems, $C(1 - C) \sim C_0(1 - C_0)$, was used in the last term for the mass flux, see eq. (1). The study is focused at the mixture with positive Soret effect $S_T > 0$. In this case the temperature gradient and the flux due to thermodiffusion have the same direction, so the chosen denser component is driven by thermodiffusion towards the hot wall. The following boundary conditions are imposed:

Constant temperature on top and bottom walls:

$$z = 0 : T = T_{\text{cold}}, \quad z = L : T = T_{\text{hot}}.$$

The lateral walls are thermally insulated:

$$x = 0 \text{ and } x = L : \quad \partial T / \partial x = 0.$$

On the rigid cell boundaries the mass flux should vanish and then the relations between concentration and temperature variations are similar to that in eq. (2)

$$\nabla C = -S_T C(1 - C) \nabla T. \quad (5)$$

Equations (3) and (4) have one way coupling. From eq. (5) it follows that $\nabla C = 0$ on the lateral walls. So, even if we consider the problem in finite size cell, the obtained results are similar for an infinite layer.

Initial conditions at $t=0$: $T = T_{\text{mean}}$, $C = C_0 = 0.5$.

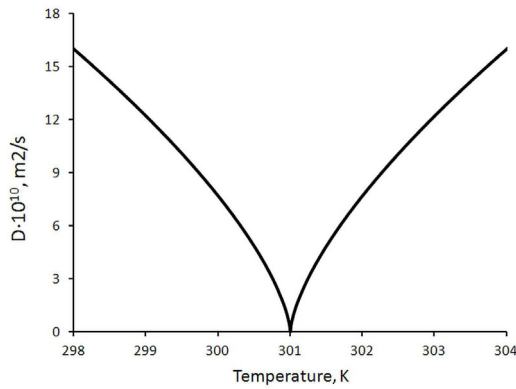


Fig. 2. Dependence of the diffusion coefficient on temperature, $T_{cr} = 301$ K.

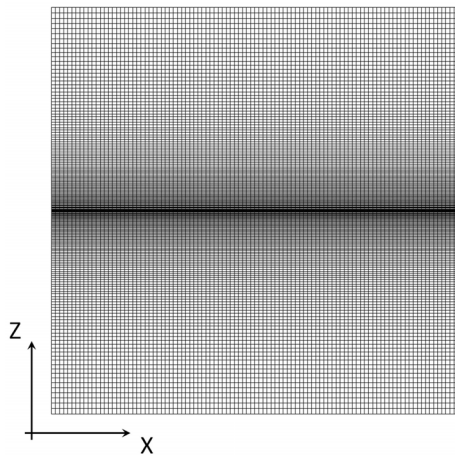


Fig. 3. Computational mesh for the case when $T_{cr} = T_{mean}$.

In the considered model liquid all the phenomenological coefficients are assumed to be constant except for diffusion D . Following the theoretical predictions [2], the diffusion coefficient obeys a power law with an exponent $2/3$ close to critical temperature

$$\begin{aligned} D(T) &= D_0 \left[D^* + \alpha \left(\frac{|T - T_{cr}|}{T_{cr}} \right)^{2/3} \right] \\ &= D_0 \left(D^* + \alpha |\epsilon|^{2/3} \right). \end{aligned} \quad (6)$$

The absolute value of $|\epsilon|$ is used in eq. (6) because the critical behavior of the diffusion coefficient is the same below and above T_{cr} . Figure 2 presents the variation of the diffusion coefficient with temperature around the critical point. The value D^* in eq. (6) is very small and is used to avoid numerical instability at the critical point, $D^* \sim 10^{-3}$. The coefficient $\alpha = 21.2522$ is chosen in a way that at $T = 298$ K the diffusion coefficient is equal to $D_0 = 1.6 \cdot 10^{-10} \text{ m}^2/\text{s}$, see table 1.

We use a numerical approach similar to that one developed in [13] using the commercial solver FLUENT v.6.3. Computations in system with strong gradients require complicated computational mesh. The mesh was gener-

ated by the commercial code GAMBIT and for the case when $T_{cr} = T_{mean}$ is shown in fig. 3. The results were obtained using 100×200 grid points on non-uniform mesh for z -axis. The mesh has stretched factor 0.975 toward the critical point. A new mesh was generated for each spatial location of the critical temperature. Numerical simulations using mesh without stretching were also conducted in the same computational domain for a different number of grid points but the results were grid-dependent.

3 Results

In the absence of bulk motion, the joint action of the Soret and diffusion processes leads to the establishing of a linear concentration profile similar to that of the temperature. Here, however, we show that unexpectedly non-linear separation of the components between cold and hot walls can occur due to presence of critical region.

The most intriguing issue in the development of the Soret separation is the choice of the critical temperature T_{cr} with respect to the temperature of the cold and hot walls. If $T_{cr} < T_{cold}$ then the results are suitable for the consolute and plait critical points. In the case when $T_{cold} < T_{cr} < T_{hot}$ the study can be valid only for the plait point.

3.1 Critical point outside of the applied temperature range, either $T_{cr} > T_{hot}$ or $T_{cr} < T_{cold}$

In this section we consider that critical point is above the temperature of the hot wall, $T_{cr} > T_{hot}$. This case is similar to the problem of the components separation in ordinary mixtures with temperature-dependent diffusion.

As soon as a constant temperature difference is imposed to the horizontal walls, the concentration fronts originate at the boundaries and propagate into the bulk. The temperature field reaches rapidly a steady state, the thermal characteristic time is $\tau_{th} = L^2/\chi \sim 10$ min. Although the diffusion is much slower than the transfer of heat (by the order of inverse Lewis number $Le^{-1} = \chi/D$), in the first instants a substantial concentration field develops in the vicinity of the solid walls. The condition of zero mass flux at the solid walls (eq. (5)) results in a rapid concentration change near the walls.

Figure 4 compares the evolution of the concentration profiles in ordinary mixture (dashed curve) and mixture with the critical point (solid curve) when $T_{hot} = 298$ K. The left plot illustrates that at time $t = 3$ h the concentration near the hot side is larger for $D = D(T)$ than for $D = D_0$. However, on the cold side the concentrations are equal in both cases as $D(T) \approx D_0$. The difference between concentration profiles advances with time as can be seen by comparing the curves at $t = 3$ days (right plot). As expected, the profile $C(z)$ is linear for ordinary mixture (dashed curve) while critical separation has a substantial effect on the shape of the concentration profile, even at temperatures well below T_{cr} .

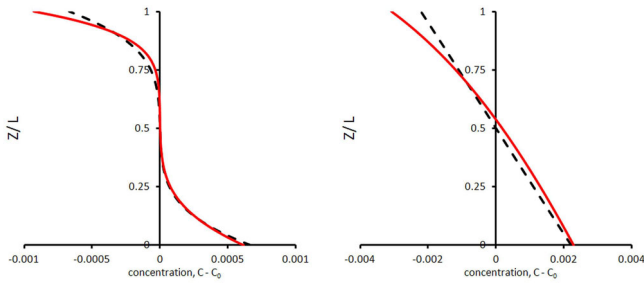


Fig. 4. Concentration profiles at $t = 3$ h (left) and $t = 3$ days (right) when $(T_{\text{cr}} - T_{\text{hot}}) = 3$ K; $D = D_0$ (dashed curves) and $D = D(T)$ (solid curves).

The five curves in fig. 5 show the components separation between walls $\Delta C = (C_{z=L} - C_{z=0})$ with time at different distances from the critical point. With the decrease of $(T_{\text{cr}} - T_{\text{hot}})$ the components separation progresses faster at the short time scale and attains a larger value at the steady state. When the temperature difference between the hot wall and the critical point is reduced from 3 K to 0.1 K, the separation increases by almost 3 times: from $\Delta C = 0.0035$ to $\Delta C = 0.0093$. The growth rate of ΔC also increases with approaching the critical point.

3.2 Critical point inside of the applied temperature range, $T_{\text{cold}} \leq T_{\text{cr}} \leq T_{\text{hot}}$

To set the base of the discussion that follows we begin our study by considering the case $T_{\text{cr}} = T_{\text{mean}}$, *i.e.* the critical temperature is in the middle of the cell. On a short time scale (τ_{th}), the concentration fronts progressively expand from the walls to the interior driven by the Soret effect. Figure 6(a) shows that at $t = 3$ h the mixture in the central part of the cell still keeps the initial concentration C_0 while near the walls the concentration fronts are well developed. Two concentration distributions $C(z)$ across the cell, dashed curve for $D = D_0$ and solid curve for $D = D(T)$, are similar in fig. 6(a). The concentration on the walls is slightly larger for the case of variable diffusion coefficient, because the proportionality coefficient ($\sim 1/D$) in the boundary condition (eq. (5)) is larger.

An unusual behavior associated with the critical point starts to be visible one day after the beginning of the Soret separation, see fig. 6(b). The symmetric concentration fronts moving from the opposite walls come into contact at the region where the diffusion coefficient has its smallest value, *i.e.* asymptotically vanishing. The separation of the components, driven by the linear temperature gradient, continues but remixing slows down due to weak diffusion. Consequently, a horizontal plateau is formed in the middle of the cell where the plane $T = T_{\text{cr}}$ tends to block the diffusion flux.

Figure 6(c)-(d) illustrates that over time the plateau advances in horizontal direction leading to a significant increase of the concentration difference between cold and hot walls in comparison with mixture without critical point, as seen from comparison of dashed and solid curves. The

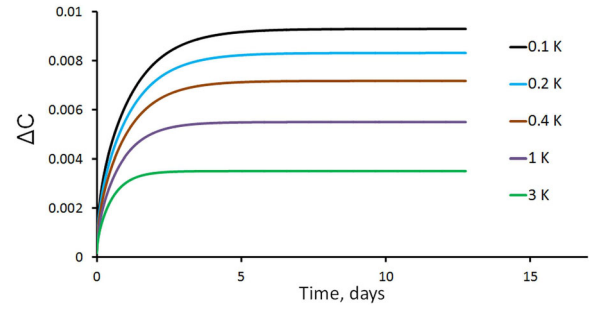


Fig. 5. Soret separation approaching the critical point. The values $(T_{\text{cr}} - T_{\text{hot}})$ are written on the plot.

increase of the components separation can be expected as the Soret coefficient strongly increases with the decrease of diffusion, $S_T \sim 1/D$. This striking behavior is observed over long time, and the concentration profile keeps the shape with horizontal plateau at the steady state. Note, that in the case of $D = D_0$ the concentration distribution approaches a linear profile, similar to that of the temperature during one day. The large difference in the time constants is a consequence of working close to a critical point (critical slowing down). A narrow and sharp concentration profile formed due to heating by a laser beam was observed in polymer blends near the consolute critical point [14].

The concentration field in the entire cell is shown in fig. 7 in the steady-state regime. In the case of ordinary mixture, $D = D_0$ (left plot) the concentration linearly decreases from the hot to the cold side. The presence of the critical point (right plot) redistributes the concentration field, it creates in the critical region a narrow zone with a sharp change in the concentration, which is seen as horizontal plateau on vertical profiles. Strong concentration gradients are established across this layer. The effect of varying the position of the critical temperature between the hot and cold walls on the dynamics of mixture separation is investigated next. Remind that T_{cr} is constant (301 K) and here T_{hot} and T_{cold} are changed. Figure 8 shows the vertical concentration distribution for seven different positions of the critical point: one of them is the case considered above when T_{cr} is in the middle of the cell when $T_{\text{mean}} = 301$ K (dashed-dotted curve) and three curves below and three curves above corresponds to the variation of T_{mean} with step $\delta T = 0.5$ K. The temperature distribution becomes linear at relatively early times (~ 15 min) while the concentration profiles are shown at $t = 50$ days. On the basis of the linear temperature distribution, the locations of T_{cr} inside the cell are shown by large dots on the vertical axis while the values of the mean temperature are written on the plot. All the curves with critical point in the interval $T_{\text{cold}} < T_{\text{cr}} < T_{\text{hot}}$ exhibit a concentration plateau at z -location of T_{cr} . The decrease of T_{cr} from the hot side (when $T_{\text{mean}} = 299.5$ K) shifts the plateau down and its center is displaced to the right with respect to the initial concentration C_0 . This leads to the development of the pattern shown in fig. 8 when the set of similar shape curves forms a “critical separation road”.

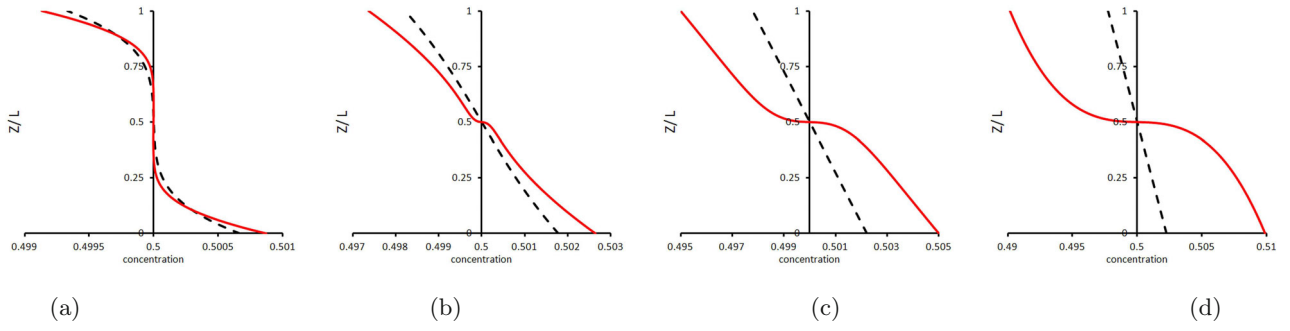


Fig. 6. The concentration profiles $C(z)$ at different time instants: (a) $t = 3$ h; (b) $t = 1$ day; (c) $t = 3$ days; (d) $t = 20$ days. Dashed curve corresponds to constant diffusion coefficient D_0 ; solid red curve corresponds to $D = D(T)$ when $T_{cr} = T_{mean}$, $\Delta T = 3$ K.

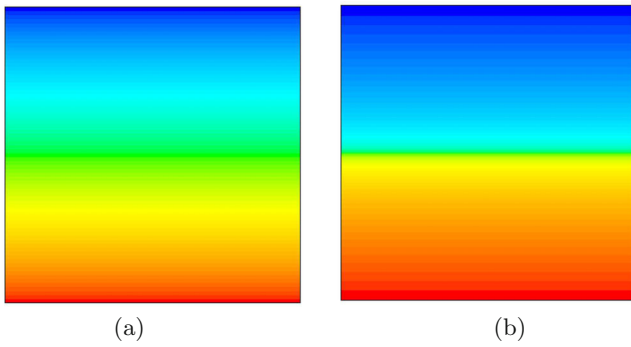


Fig. 7. Concentration field after (a) 3 days separation with constant diffusion coefficient $D = D_0$; (b) 50 days separation when D follows eq. (6). (Each plot consists of 70 levels of concentration and these levels are the same at both plots.)

These curves also show that in the critical region with asymptotically small diffusion the concentration gradient ($\partial C/\partial z$) tends to infinity at $T = T_{cr}$. The dashed curves, in which T_{cr} is equal either to T_{cold} or T_{hot} , present half of the horizontal plateau on the interior curves. Imaginary shifting the curve with ponding $T_{mean} = 302.5$ K (when T_{cr} is on the cold wall) would form the horizontal plateau. Note that these surprisingly narrow and sharp concentration layers are induced by a broad temperature distribution.

Figure 9 shows the time evolution of the concentration difference (*i.e.* the Soret separation) between hot and cold walls, $\Delta C = C_{z=L} - C_{z=0}$. The figure comprises the same seven curves shown in fig. 8 but only four are visible. Curves on which T_{cr} is symmetric with respect to the cell center are overlapped: $T_{mean} = T_{cr} \pm \delta T$ (curve 2); $T_{mean} = T_{cr} \pm 2\delta T$ (curve 3). Consequently, curve 1 presents separation when T_{cr} is in the middle of the cell and curve 4 when T_{cr} is equal to the temperature of one of the solid walls. Identical behavior of the separation curves symmetric with respect to the location of T_{cr} to the cell center is not surprising. It is associated with the temperature dependence of the diffusion coefficient which is symmetric with respect to T_{cr} as seen from fig. 2.

The unexpected result is that the separation ΔC in the steady state does not depend on the location of T_{cr}

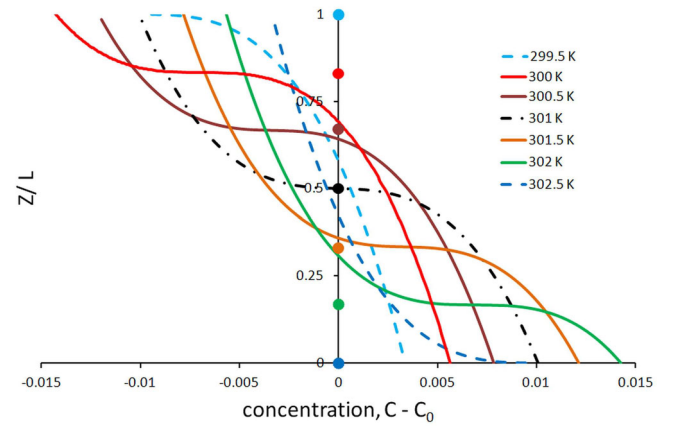


Fig. 8. Critical separation road: concentration profiles over the cell height after 50 days of separation. Different curves correspond to various locations of T_{cr} between T_{hot} and T_{cold} . The values of T_{mean} are written on the plot, $\Delta T = 3$ K.

inside the major part of the cell. The separation first undergoes a strong transient period ($t < 10$ days) and then slowly approaches a steady value. At the earlier times the growth rate of the separation depends on the location of the critical point: the smaller the difference between T_{cr} and the temperature of the closest wall, the larger the growth rate. After ≈ 25 days all the curves in fig. 9 attain the same asymptotic value.

Another noteworthy result is the strong increase in the separation as soon as the critical point is placed in the interior of the cell. Indeed, in the case when T_{cr} is on the bounding walls (curve 4) $\Delta C_{wall} = 0.0128$, while for all other curves in fig. 9 separation is almost twice larger, $\Delta C_{interior} = 0.0201$. However, we noticed that when the location of T_{cr} approaches from inside to the wall as close as $z/L \approx 0.015$, the separation starts decreasing sharply. Comparison of fig. 9 and fig. 5 shows that ΔC continues to decrease below ΔC_{wall} when T_{cr} is outside of the cell, *i.e.* above the temperature of the hot wall.

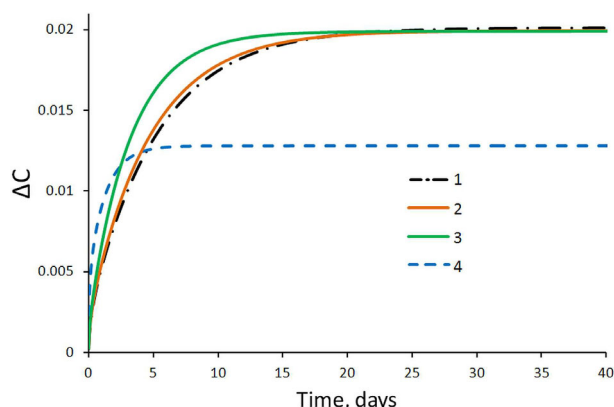


Fig. 9. Evolution of the Soret separation ΔC with time for different locations of T_{cr} between T_{hot} and T_{cold} . Curve 1 presents separation when T_{cr} is in the middle of the cell and curve 4 when T_{cr} is equal to the temperature of one of the bounding walls, $\Delta T = 3$ K.

4 Conclusions

In the present work, we performed an extensive computational study of the kinetic of the components separation in a model binary mixture with critical point and compared the results with that of an ordinary mixture. In order to isolate the effects of an asymptotic behavior of mass diffusion in a critical region, the thermal diffusivity χ is assumed to be constant.

Our analysis identified that, unlike ordinary mixtures, non-linear concentration profile across the cell is established in a steady state due to presence of a critical region. A thin layer, associated with strong concentration gradient $\partial C/\partial z$, forms in the critical region.

The Soret separation occurs in the mixture in the presence of a temperature gradient and the definition of “distance” to the critical temperature is ambiguous. The difference ($T_{cr} - T_{hot}$) was used as a control parameter measuring the distance to the critical point. Replacing T_{hot} by T_{cold} does not provide any quantitative changes as $\Delta T = 3$ K and is constant throughout the study.

We show that the kinetic of the separation depends not only on the distance to the critical point but also on the location of the critical point: inside or outside the

Soret cell. When T_{cr} is outside the cell (*e.g.*, $T_{cr} > T_{hot}$) the Soret separation in a steady state continuously increases with diminishing the difference $T_{cr} - T_{hot}$. A surprising finding is that, if T_{cr} is inside the cell, then the Soret separation does not depend on the location of T_{cr} between the hot and cold walls. A sharp decrease in the separation occurs when T_{cr} is extremely close to the bounding walls. Furthermore, the value ΔC is almost twice as large in the case when T_{cr} is inside the cell than when T_{cr} is outside the cell.

Let us note that we have used a simplified model. Other models taking into account the critical behaviour of thermal diffusivity could be investigated in future studies along the same lines.

References

1. J.V. Sengers, J.M.H. Levelt Sengers, *Annu. Rev. Phys. Chem.* **37**, 189 (1986).
2. J. Luettmer-Stathmann, in *Lecture Notes in Physics*, edited by W. Köhler, S. Wiegand, Vol. **584** (Springer, Berlin, 2002), p. 24.
3. W. Köhler, A. Krekhov, W. Zimmermann, *Adv. Polym. Sci.* **227**, 145 (2010).
4. P. Bergé, M. Dubois, *Phys. Rev. Lett.* **27**, 1125 (1971).
5. A. Mialdun, V. Shevtsova, *J. Chem. Phys.* **134**, 044524 (2011).
6. A. Mialdun, V. Sechenyh, J.C. Legros, J. Ortiz de Zárate, V. Shevtsova, *J. Chem. Phys.* **139**, 104903 (2013).
7. M. Giglio, A. Vendramini, *Phys. Rev. Lett.* **34**, 561 (1975).
8. A. Mialdun, C. Minetti, Y. Gaponenko, V. Shevtsova, F. Dubois, *Micrograv. Sci. Technol.* **25**, 83 (2013).
9. V. Shevtsova, C. Santos, V. Sechenyh, J.C. Legros, A. Mialdun, *Micrograv. Sci. Technol.* **25**, 275 (2014).
10. W.M. Rutherford, J.G. Roof, *J. Chem. Phys.* **63**, 1506 (1959).
11. O. Ecenarro, J.A. Madariaga, J.L. Navarro, C.M. Santamarfa, J.A. Carrión, J.M. Savirón, *J. Phys.: Condens. Matter* **5**, 2289 (1993).
12. A. Mialdun, V. Shevtsova, *C. R. Mec.* **339**, 362 (2011).
13. V. Shevtsova, Y. Gaponenko, A. Nepomnyashchy, *J. Fluid Mech.* **714**, 644 (2013).
14. A. Voit, A. Krekhov, W. Köhler, *Phys. Rev. E* **76**, 011808 (2007).